AD-A072 709 GENERAL MOTORS CORP INDIANAPOLIS IND DETROIT DIESEL --ETC F/G 21/5
LASER ANEMOMETER MEASUREMENTS AT THE EXIT OF A T-63-C20 COMBUST--ETC(U)
APR 79 D R ZIMMERMAN NAS3-21267
UNCLASSIFIED DDA-RN-79-4 NASA-CR-159623 NL

| OF |
ADA
072709

END
DATE
FILMED
9-79
DDC

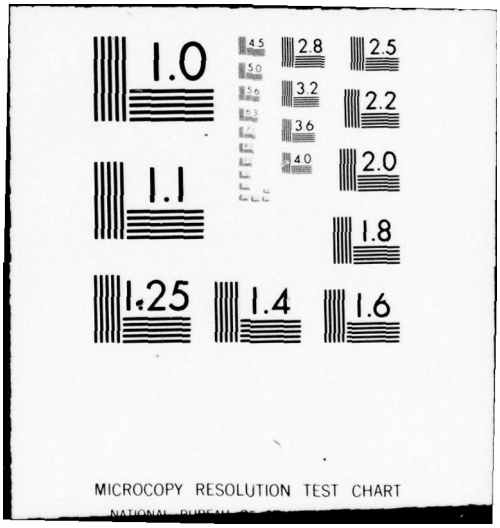
1.0
1.1
1.25
1.4
1.6
1.8
2.0
2.2
2.5
2.8
3.2
3.6
4.0
4.5
5.0
5.6
MICROCOPY RESOLUTION TEST CHART

LEVEL II

NASA CR-159623
DDA RN 79-4

LASER ANEMOMETER MEASUREMENTS AT THE EXIT OF A T63-C20 COMBUSTOR

by D. R. Zimmerman

DETROIT DIESEL ALLISON

prepared for

NATIONAL AERONAUTICS AND SPACE ADMINISTRATION

NASA Lewis Research Center

Contract NAS 3-21267

1. Report No.	2. Government Accession No.	3. Recipient's Catalog No.
NASA CR-159623		

4. Title and Subtitle
LASER ANEMOMETER MEASUREMENTS AT THE EXIT OF A T63-C20 COMBUSTOR

5. Report Date
April 1979

6. Performing Organization Code

7. Author(s)
D. R. Zimmerman

8. Performing Organization Report No.
DDA-RN-79-4

10. Work Unit No.

9. Performing Organization Name and Address
Detroit Diesel Allison
Indianapolis, IN 46206

11. Contract or Grant No.
NAS3-21267

13. Type of Report and Period Covered
Final Contractor Report
Sept. 1978-April 1979

12. Sponsoring Agency Name and Address
Propulsion Laboratory
US Army Research & Technology Laboratories (AVRADCOM)
Lewis Research Center
Cleveland, Ohio 44135

14. Sponsoring Agency Code
1L162209AH76

15. Supplementary Notes
Project Manager, Edward J. Mularz, NASA-Lewis Research Center and USARTL Propulsion Laboratory (AVRADCOM), Cleveland, Ohio 44135

16. Abstract

An experimental study of the flow downstream of a T63-C20 gas turbine engine combustor was performed.

Laser anemometer measurements of the mean and fluctuating velocities were made in a Combustion Rig across an annulus simulating the inlet to a turbine.

A window design suitable for similar measurements in a gas turbine engine was made based on the results of this experiment.

Insufficient numbers of naturally-occurring scattering particles were present in the flow. Hollow phenolic particles added to the flow provided adequate signal strength for measurement.

For each of the simulated engine operating conditions of Flight Idle, 30% Power and 90% Power, both with and without the addition of fuel, the mean velocities and turbulent intensities were uniform across the annulus.

The turbulent intensity was substantially unaffected by the addition of fuel but was apparently only dependent on the inlet flow condition at a given power point.

Little or no swirl was present in the flow at the annulus.

This experiment was performed in the Combustion Research Laboratory of Detroit Diesel Allison during the Spring of 1979.

17. Key Words (Suggested by Author(s))	18. Distribution Statement
Laser Anemometer Combustion Turbulent Flow	Unclassified - unlimited

19. Security Classif. (of this report)	20. Security Classif. (of this page)	21. No. of Pages	22. Price*
Unclassified	Unclassified		

* For sale by the National Technical Information Service, Springfield, Virginia 22161

NASA-C-168 (Rev. 10-75)

019200

TABLE OF CONTENTS

LIST OF TABLES

LIST OF FIGURES

SUMMARY

The objectives of this experiment were to

1) evaluate a window design suitable for laser anemometer (LDA) measurements in the combustor exit region of a T63-C20 engine

2) determine the requirement for the addition of light-scattering particles to permit LDA measurements

3) make LDA measurements of the mean and fluctuating velocities in a combustion rig which simulates the operating conditions of a gas turbine engine.

This work included

1) evaluation of a prototype gas-cooled window which permitted optical access to the combustor exit region

2) design of a window similar to the prototype suitable for measurements in a T63-C20 engine

3) determination of a suitable seeding material and a technique for introducing the seed into the flow which produced a minimal disturbing influence on the flow

4) measurements of the mean velocity and turbulent intensity profiles across an annulus at the combustor exit for four operating conditions, both with and without the addition of fuel.

As a result of this experiment, it was determined that

1) a suitable window design has been achieved and a cooling flow of 0.028 m^3/min was sufficient to adequately cool and cleanse the window for up to 3 hrs. of operation at the Flight Idle condition (which produced the most soot)

2) a fluidized bed of hollow phenolic particles was required to give sufficient scattered light for LDA measurements with a counter-processor

3) the profiles of mean velocity and turbulent intensity were uniform across the annulus and at a prescribed inlet condition the turbulent intensity was relatively unaffected by combustion.

The principal conclusions concerning the fluid dynamics of the flow in the annulus were

1) the mean velocity and turbulent intensity profiles were essentially uniform at each operating condition

2) the non-burning, or isothermal, turbulent intensity increased with increasing Reynolds number

3) the turbulent intensity appeared to be only a function of the inlet conditions and was not appreciably changed by combustion

4) little or no swirl was present in the flow.

INTRODUCTION

It has been shown by a number of experiments(1,2,3) that forced convective heat transfer is strongly dependent on the freestream turbulent intensity of the flow. It thus becomes a parameter of importance in the design of cooled devices and in modeling heat transfer experiments.

The particular application which gave impetus to the present experiment is the interaction between the hot gas flow leaving a gas turbine engine combustor and the cooled turbine vanes located just downstream of the combustor.

Very few experiments have been performed which apply to the geometry under consideration here. Shafter, Koch and Pfeifer(4) using a forward-scatter LDA system to measure the flow from a jet engine combustor found particles suitable for scattering but had to add additional scattering particles to increase the data rate to an acceptable level. They measured periodic maxima in mean velocity around an annulus associated with the 20 injectors located upstream. A minimum turbulent intensity of 12% was measured at each of the mean velocity maxima. They also performed an experiment in high-temperature, supersonic flow which showed that negligible errors were introduced in the measurements of the mean and turbulent velocities by variations in the refractive index of the gas.

Eckert, Goldstein and Sparrow(5) found that the turbulent kinetic energy level in isothermal flow was unchanged by combustion however the turbulent intensity was reduced by 50% since the mean velocity was doubled. In contrast, Driscoll and Pelaccio(6) found no change in turbulent intensity with combustion.

Edelman and Harsha(7) in a very comprehensive review of combustor gas dynamics concluded that

1) The flow downstream of sudden expansions, fuel nozzles, central recirculation zones and combustion zones in many instances have large-scale, time-dependent fluctuations which may void the usual assumption of stationarity

2) the effect of combustion may be to increase or decrease the isothermal turbulent intensity depending on the predominant phenomena among the competing effects of dilation or mean velocity divergence, shear stress generation by local velocity gradients, recirculation imparted by the swirl passages and the configuration of the combustion zone

3) when swirl is added to stabilize the central recirculation zone, the tangential velocity component downstream of the swirl vanes decays quite rapidly

4) each combustor is an entity and little if any correlation between or among combustors is possible.

The scope of the present work involved mapping the flow across a simulated turbine nozzle entrance in a steady flow combustion rig for several operating conditions of the combustor both with and without fuel addition. The combustor liner-fuel nozzle combination were typical of the T63-C20 gas turbine engine. The fuel was JP-5. The simulated engine power conditions were Flight Idle, 30% Power, 90% Power and Take Off. Traverses were made across the annulus as close to the bounding surfaces as flare (background radiation) would permit.

This experiment has defined the T63-C20 combustor exit flow field. Very few results have been published previously of LDA measurements in combustor exhausts. Techniques were developed for obtaining LDA traverse data and determining the mean and variance from a velocity histogram.

Although the photomultiplier signals had a relatively low signal to noise ratio, compared to an open jet, the significance of the findings are threefold.

1) The designer of T63-C20 or similar cooled turbine vanes now has better values for the free-stream turbulent intensity than previously available as well as a verification of the mean velocity field entering the turbine.

2) The experimenter performing T63-C20 or similar heat transfer modeling experiments has values he can use to adjust the flow in his cascade tunnel.

3) A basis for comparison has been established for similar measurements in a T63-C20 engine experiment. If the engine

measurements agree satisfactorily with the data obtained here, the less expensive rig tests may be used to evaluate the combustor exit flow.

The specific purposes of this experiment were to

1) Evaluate a window design which could be used to provide optical access to the combustor exit region of a gas turbine engine

2) Determine if additional light-scattering particles would be required to obtain LDA measurements

3) Map out the velocity field at the combustor exit for a number of operating conditions.

The experiment was performed at the Detroit Diesel Allison Combustion Research Laboratory in the T63 Combustion Rig.

An optical access port containing a cooled sapphire window was mounted in a spoolpiece located in the region just downstream of the combustor. This spoolpiece and a centerbody defined the annulus which simulated the turbine inlet.

Additional scattering particles were required for LDA measurements. These particles were added to the flow from a fluidized bed of hollow phenolic particles.

A laser anemometer was assembled on an optical table mounted on a milling machine equipped with stepping motors. The configuration established for this experiment was 15 degrees off-axis backscatter. The photomultiplier signals were demodulated by a counter processor. The counter data were stored, tabulated and analyzed on-line with a digital computer. Further analysis of the counter data was performed off-line with computer-graphics.

EXPERIMENT

Apparatus

The combustor under test in this experiment was a standard T63-C20 combustor liner and a standard T63-C20 fuel nozzle. The fuel used was JP-5.

The T63 Combustion Rig (Figure 1) was attached to a source of compressed air capable of supplying 0.91 to 4.55 kg/s at 689 kPa or up to 2.27 kg/s at 2068 kPa. Combustor test section mass flow and pressure were controlled by inlet and exit valves. Inlet air temperature was controlled with in-line electric heaters. An upstream orifice meter was used to monitor the air mass flow.

Four pressure probes were used to monitor the combustor inlet total pressure and two thermocouples were used to monitor the inlet temperature.

In the spoolpiece at the combustor exit (Figure 2), two total pressure probes and 20 thermocouples were mounted in a circumferential array to monitor the pressure drop across the combustor and the combustor exit temperature profile. Fuel pump pressure and fuel flow were also continuously monitored.

The measurements of these parameters were acquired and tabulated by a high-speed laboratory digital computer. An uncertainty analysis of the rig operation (Appendix A) led to the conclusion that the bulk flow velocity was constant, typically within 0.5% during the acquisition of an LDA measurement (5 to 15 minutes) and further that the bulk flow velocity was constant to within about 0.5% for all the measurements in a profile at a given operating condition — even though some measurements were made several weeks apart. The repeatability and control of the Combustion Rig pressure, temperature and mass flow were deemed highly satisfactory.

A gas-cooled optical access port (Figure 3) was mounted in the side of the instrumentation spoolpiece to permit LDA measurements in the annulus defined by the internal diameter of the spoolpiece and a centerbody.

The laser anemometer was assembled on an optical table in a 15 degree off-axis backscatter configuration (Figure 4). A large backscatter angle improves the radial resolution however the window and window mount limited the backscatter angle to 15 degrees. The argon-ion laser was operated in the single wavelength mode at 5145 Å and 0.100 watts. A cube-type beam splitter was used to give two equal intensity parallel beams spaced 20 mm apart. These two beams were brought to focus at the measurement volume by a 750 mm focal length, f/4.3 positive lens.

Light scattering particles were added to the flow from a fluidized bed of hollow phenolic particles. To prevent back-pressuring the fluidized bed, a valve was placed in the output line of the seeder. The seeder output passed through the external dome of the combustor rig and along the outer surface of the combustion liner. The tube was welded in place through a hole in the liner (Figures 5 and 6) permitting the seed material to enter the interior of the liner and mix with the combustion gas in the horizontal plane of the optical access window approximately 85 mm upstream. The nitrogen flow rate through the seeder was approximately 0.010 m^3/min.

The scattered light from the measurement volume was collected by a 210 mm, f/1.5, compound receiving lens equipped with an internal

iris and focussed on a 275μm aperture in front of a photomultiplier tube. The photomultiplier output was amplified by a preamplifier and transmitted to a counter processor in the control room. The counter processor output was stored, tabulated and analyzed by an on-line laboratory digital computer. Subsequent analysis of the LDA data was performed off-line on a computer graphics terminal.

Procedure

The laser+beam splitter+transmitting lens combination used in this experiment gave a measurement volume 0.33 mm diameter and 24.6 mm length with a 19.3μm fringe spacing. One design consideration in a laser anemometer is to ensure that the beam waists coincide with the center of the measurement volume, i.e. the two beams which are being focussed both have a minimum diameter at the point in space where they are brought together. If they do not, one obtains a variable fringe spacing along the measurement volume length leading to broadening of the velocity spectrum. Since this phenomena is primarily a problem caused by the spherical aberration of the transmitting lens, one approach is to use a large diameter lens and a small beam separation, utilizing only the center of the lens. In this experiment a transmitting lens of 175 mm diameter was used with a beam separation of 20 mm. Verification of the coincidence of the beam waists with the measurement volume center was established in an earlier experiment described below.

Uniform flow was established in a 76 x 76 mm duct, the measurement volume of length 24.6 mm was centered in the duct and the image of the measurement volume length was scanned with a 0.200 mm aperture. The measured mean velocity and turbulent intensity were uniform to within 1% over the center 16.2 mm of the measurement volume implying a constant fringe spacing over this length. During the course of this verification experiment, a technique was developed for traversing the width of a small channel in both forward and backscatter which obviates the problems associated with moving the entire laser anemometer system. To traverse any flow channel of width approximately 17 mm or less, one merely centers the LDA measurement volume in the channel, images the measurement volume with a collecting lens on a movable aperture plate in front of a photomultiplier tube and scans the image by translating the aperture with a micrometer drive (Figure 7). This technique was used to advantage in the present experiment where the annulus height was 14.2 mm.

Figure 4 indicates the position and orientation of the various components of the LDA system. In this configuration the image length of the measurement volume, projected on the aperture plate

was 1/10 the object length, i.e. the annulus height of 14.2 mm was imaged to 1.42 mm. The image length of 1.42 mm and an aperture diameter of 0.275 mm permitted 5 discrete, non-overlapping measurement regions in making a traverse across the annulus height.

By far the greatest impediment to making LDA measurements in a narrow channel is the background light, in this case, the reflected light from the window and from the centerbody. The reflected light gives rise to a significant current in the photomultiplier representing a noise level which can in some instances exceed the signal level from the scattered light from the seed particles. The procedure followed here to reduce the noise generated by reflected light was to

(1) Mask the transmitting lens to pass only the two converging beams and block the light internally scattered in the beam splitter. The beam splitter is a bright, potential noise source whose image is projected through the transmitting lens onto the side of the combustion rig unless masked.

(2) The window was slightly recessed from the outside diameter of the annulus moving the reflection from the window out of the range of measurement.

(3) A 3.18 mm diameter hole was drilled in the centerbody which effectively eliminated the reflection from the centerbody.

These precautions were sufficient to yield a signal to noise ratio (S/N) of 4 to 5 under a majority of operating conditions, at least until the window was too dirty to transmit the particle-scattered light.

The LDA was aligned by adjusting the collecting lens, aperture plate and photomultiplier with the measurement volume located in free space. The milling machine was then moved into position so that the measurement volume was located in the annulus. The presence of the 3.2 mm thick sapphire window moved the center of the measurement volume away from the LDA an estimated 1.4 mm. The final alignment was made by translating the LDA until a reflection from the centerbody was centered on the aperture and then translating the LDA away, 7.1 mm, to the center of the annulus. Traverses were then made from this location by moving the aperture along the measurement volume image length with a micrometer drive.

The T63 Combustion Rig is cantilevered from the exhaust duct-work through a large bellows located to the right and not visible in Figure 1. The combustor is thus free to move in space subject to differential thermal expansion, internal air pressure

and internal water pressure (coolant for the exhaust gas downstream of combustor). This movement necessitated realignment of the LDA after stability was achieved at a given combustor operating condition.

Two closed-circuit television units were used to monitor the location of the transmitted beams with respect to the window and the location of the aperture with respect to the measurement volume image. These monitors, in conjunction with the milling machine stepping motor controllers, permitted remote alignment of the LDA with respect to the combustion rig.

Since the counter processor needed to be located in close proximity to the control room computer, this required that the photomultiplier output be transmitted through approximately 12 meters of coaxial cable. To eliminate line losses and a decreased S/N, the photomultiplier output was amplified by an LDA tracker preamplifier before transmission to the counter. This increased the flexibility of the data acquisition process since both the preamplifier gain and the counter threshold could be varied independently to optimize the data rate.

Since the S/N is dependent on the photomultiplier voltage and laser power as well as the background light and characteristics of the scattering particles, it was necessary to constantly monitor the photomultiplier output, the preamplifier output and the data rate during the acquisition of a set of particle velocities. Typically, a set of 1000 particle velocities are acquired to generate a histogram defining the mean velocity and turbulent intensity at a point. The iris in the collecting lens proved invaluable in optimizing the S/N. Usually, stopping down the collecting lens from f/1.5 to f/8 gave a respectable S/N of 4 to 5.

The only foolproof validation technique for assessing whether the counter is acquiring information from good Doppler signals or counting primarily noise is to observe the frequency with which good particle velocity bursts appear on an oscilloscope and adjust the preamplifier gain and counter threshold such that the data rate is equal to or less than this frequency of occurrence. For the majority of the data taken here, the data rate was 1 to 3/sec or 5 to 15 minutes/1000 particle velocities. This constant monitoring and adjustment to maintain the proper data rate required that most of the experiment time be spent near the combustion rig. The conditions of 90% and Take-Off with fuel addition were considered too dangerous to permit habitation of the test cell and remote operation was attempted. In addition to an inability to remotely optimize the S/N, the 90% and Take-Off conditions gave a considerable background of radiation from the flame. Insertion of a 5145 Å line filter

resulted in loss of the particle scattered signals. The preceding factors contributed to uncertainties in the measured velocities at these two conditions. At the Take-Off condition, the level of background light and pulsations in mean velocity prevented determination of the turbulent intensity.

The 20 mm beam splitter was mounted in a rotational stage which permitted measurements at $\pm$ 45°. These data combined with the axial flow measurement yielded the tangential velocity in the annulus. In addition to the LDA measurements, single-wire, hot-wire measurements were in the annulus at room temperature.

The seeder, a fluidized bed of hollow phenolic particles (Figure 8) was connected to a tank of dry nitrogen through a valve which controlled the through-flow rate. The tank pressure was maintained at 25 to 30 psi above the combustor inlet pressure. An on-off valve was placed in the line between the seeder and the combustion rig to prevent back pressuring and possibly clogging the seeder.

The twelve cooling gas tubes of the window housing were connected to copper lines with compression fittings and Teflon inserts for ease of disassembly. The copper tubes were connected to a common manifold pressurized by a tank of dry nitrogen. The tank pressure was maintained slightly greater than the static pressure in the annulus-sufficient to maintain a cooling gas flow of about 0.028 m^3/min.

Results and Discussion

The window used to permit optical access of the LDA to the simulated turbine nozzle region of the T63 Combustion Rig has proved quite adequate. A cooling gas flow of 0.028 m^3/min of dry nitrogen was sufficient to provide cooling and cleansing of the window. The worst operating condition in terms of soot formation and deposition was Idle-Burning. Under these conditions, operation was limited to about three hours before an excessive amount of soot accumulated on the window and disassembly and cleaning was required. Cleaning was accomplished by successive washings with ethanol and rubbing with a rubber eraser. A window design suitable for engine measurements including detail drawings and instructions for assembly, based on the results of this experiment, have been submitted under separate cover.

With the optical components and geometrical configuration of the LDA as used in this experiment (Figure 4), the S/N of the combustion generated particles was insufficient to obtain

photomultiplier signals which could be utilized by a counter-processor. A preliminary estimate of the number of combustion-generated particles in the measurement volume, based on smoke measurements, was 623. Based on this number density, an LDA tracker processor could be used to give a continuous signal directly proportional to the velocity. To get a good S/N from an LDA system requires that the interference fringe spacing be only slightly larger than the scattering particle diameter, cf. Durst, Melling and Whitelaw(8). Combustion personnel supplied the information that the solid particulates leaving the combustor were carbon with a size distribution peaking between 0.1 and 0.2μm. A fringe spacing of 0.3μm would have yielded Doppler frequencies for this experiment of $130 \leq f_D \leq 367$ MHz, out of the range of either the tracker or the counter. The advantages of having a uniform fringe spacing across what amounts to a blind hole as well as generating Doppler frequencies in the range 2 to 4 MHz led to the use of a 19.3μm fringe spacing.

Addition to the flow of hollow phenolic particles gave a S/N of 4 to 5 which permitted measurement of the particle velocities. The phenolic particles were mixed and entrained in the flow by a seeder composed of a fluidized bed and several valves (Figure 8).

Velocity measurements across the annulus simulating the turbine inlet were obtained at four combustor operating conditions (Table 1) both with and without the addition of fuel (Table 2). In addition, a single-wire, hot-wire survey was made across the annulus at room temperature.

The hot-wire measurements were made under in-draft conditions. The feed arms were disconnected from the air source and room air was pulled through gate valves preceding the feed arms using a stream ejector tied to the exhaust ductwork.

The mean velocity profile, Figure 9, indicates a uniform mean velocity across the annulus from a differential radius of 0.5 mm to 11.2 mm from the center body. The flow in the outer 3 mm of the annulus is disturbed by a shroud which extends from the combustor liner to give a smooth transition between the combustion liner and the inside diameter of the spoolpiece. The level of turbulent intensity measured with the hot wire (Figure 10) is higher than comparable measurements at the same mean velocity with the LDA, probably due to the high level of turbulence generated at the inlet by the gate valves used to adjust the mean velocity to 47 m/s.

The LDA surveys of mean velocity under both burning and non-burning conditions (Figure 11) indicated a uniform mean velocity profile under all conditions. The radial resolution of the LDA

measurements is the aperture diameter projected onto the measurement volume, i.e. 0.275 mm x 10 = 2.75 mm, approximately 20% of the annulus height.

A number of factors such as

1) leaks at the flanges and inlet feed-arms (the feed-arms are slip-fit to accommodate differential thermal expansion)

2) asymmetric distribution of area around the annulus (the result of several years of thermal cycling, cracking and weld repair)

3) asymmetric distribution of temperature around the annulus (the result of non-uniform combustion)

combined to prevent the calculation of the bulk velocity through the measurement volume from measured values of the rig parameters of temperature, pressure and mass flow.

A comparison of the ratio burning/non-burning volumetric flow rate, based on the rig parameter measurements, with the ratio burning/non-burning velocity, measured with the LDA, was made.

	$\frac{Q(\text{burning})}{Q(\text{non-burning})}$	$\frac{U(\text{burning})}{U(\text{non-burning})}$
Flight Idle	1.90	2.00
30% Power	1.91	2.01
90% Power	2.06	2.14
Take Off	2.14	2.25

The agreement is seen to be within 5% and is considered reasonable considering the uncertainties of the experiment. While the uncertainties in the volumetric flow during a velocity measurement and from point to point in an annular profile were held to about 0.5%, the absolute value of the volumetric flow was only calculable to about $\pm$ 2.5% (Appendix A).

The histograms of velocity versus the number of particles with a given velocity within a velocity bandwidth (dependent on the counter-processor resolution) were first scanned on-line to determine that an adequate number of particles were grouped about

an estimated mean velocity (Table 3). Usually, 1000 particle velocities were acquired for each histogram. The histograms were later analyzed off-line using a computer graphics terminal to determine the mean and variance which best fit the data (Appendix B).

The LDA measured turbulent intensity profiles across the annulus were in general quite uniform (Figure 12), partially because of the radial resolution of the LDA. Summarizing the data as shown in Figure 13, indicates an increase in turbulent intensity with increasing Reynolds number under isothermal conditions. This contradicts the results of Smith and Gouldin(9). Further, combustion appears to have a negligible effect on the turbulent intensity which exists in isothermal flow. This contradicts the conclusions of Eckert, Goldstein and Sparrow(5) but agrees with the results of Driscoll and Pelaccio(6).

The combustor liner of this experiment (Figures 5 and 6) is configured so that the primary air flow in the vicinity of the fuel nozzle is introduced through two sets of passages which produce a region of concentric counter-rotating flow. Measurements were made both with the LDA and a rotatable, single-wire, hot-wire probe in an attempt to determine the swirl velocity or tangential component of the mean velocity in the annulus. The LDA technique used here was to rotate the beam splitter $\pm$ 45 degrees and sum and difference the measured mean velocities as outlined in Appendix C.

The tangential velocity calculated from eqn. C.2. was less than the difference in the axial velocity determined from the $\pm$ 45 degree measurements and the 90 degree measurement, eqn. C.1. The swirl angle uncertainty due to movement of the cantilevered combustion rig was greater than 25% of the calculated value of swirl angle from eqn. C.6. It was concluded that the swirl velocity introduced in the dome of the combustor liner had decayed to a negligible value at the measurement location. This conclusion was reinforced by a rotating hot-wire survey which indicated a swirl angle less than the angular resolution of the probe and by the appearance of traces of phenolic seed and soot left on the inner and outer surfaces of the annulus which indicated an absence of swirl.

CONCLUSIONS

As a result of this experiment the following conclusions were made.

1) the mean velocity and turbulent intensity profiles across the annulus simulating the turbine inlet were essentially uniform.

2) The non-burning or isothermal turbulent intensity increased with increasing Reynolds number.

3) Combustion did not appreciably affect the isothermal turbulent intensity at a prescribed power condition.

4) Little or no swirl velocity was present in the flow through the annulus.

APPENDIX A

UNCERTAINTY ANALYSIS

The experimental uncertainties, for the purpose of discussion are separated into:

1) Uncertainties in the volumetric flow through the rig during the acquisition of an LDA histogram

2) Uncertainties in the volumetric flow from point to point in an annular traverse

3) Uncertainties in the measurement of the individual particle velocity and the ensemble averaged velocity

4) Uncertainties in the determination of the sample mean and sample variance from the velocity histograms

5) Uncertainties in the spatial location of the measurement volume.

These independent uncertainty factors are then combined to give an uncertainty in the mean velocity, turbulent intensity and corresponding spatial location.

1) The volumetric flow rate, Q, through the annulus is given by

$$Q = \frac{\dot{m}}{\rho} = \frac{\dot{m}\ R\ T}{P_s} \simeq \frac{\dot{m}\ R\ T}{(P_T - \Delta p)} \qquad (A.1)$$

Following the analysis of Kline and McClintock(10),

$$\frac{W_Q}{Q} = \left\{ \left(\frac{w_{\dot{m}}}{\dot{m}} \right)^2 + \left(\frac{w_T}{T} \right)^2 + \left[\frac{w_{P_T}}{(P_T - \Delta p)} \right]^2 + \left[\frac{w_{\Delta p}}{(P_T - \Delta p)} \right]^2 \right\}^{\frac{1}{2}} \qquad (A.2)$$

where: $\dot{m} = \dot{m} \pm w_{\dot{m}}$, $T = T \pm w_T$, $P_T = P_T \pm w_{P_T}$

and $\Delta p = \Delta p \pm w_{\Delta p}$

Evaluation of the variations $w_{\dot{m}}$, w_T, w_{P_T} and $w_{\Delta p}$ during the time interval required to obtain an LDA histogram (5 to 15 minutes) led to the conclusion that $Q = Q \pm w_Q = Q(1 \pm 0.005)$.

The absolute measurement of $\dot{m}$, T, P_T and Δp were subject to calibration errors, hysteresis and drift. These values were quoted as

$$\dot{m} = \dot{m}(1 \pm 0.02),\ T \text{ (each thermocouple)} = T(1 \pm 0.007),$$

$$P_T = P_T(1 \pm 0.01),\ \Delta p = \Delta p(1 \pm 0.002)$$

These instrument uncertainties yield absolute measurements of the flow rate $Q = Q(1 \pm 0.024)$.

Asymmetries in the annulus area caused by many hours of prior thermal cycling and asymmetries in the combustor exit temperature made calculation of the bulk velocity through the measurement volume highly speculative. The measured mean velocities are thus compared to the volumetric flow rates as indicated in the text.

2) The values of volumetric flow rate, Q_k, were tabulated for each histogram obtained at a given operating condition. For each histogram in a set of profile data, the quantity

$$\frac{\Delta Q_k}{Q_A} = \frac{Q_k - Q_A}{Q_A} \quad \text{was calculated.}$$

where:

$$Q_A = \frac{\sum_{k=1}^{\ell} Q_k}{\ell}$$

These values gave

$$Q_k = Q_A \pm \Delta Q_k = Q_A(1 \pm 0.005)$$

From the preceding analysis, it was concluded that the volumetric flow rate may be accurately determined only to within 2.4%, however variations in the flow rate are held within 0.5% while measuring the velocity and within 0.5% while making a series of profile measurements.

3) Much of the literature regarding LDA development and application has been concerned with the inherent accuracy of measuring velocities of particles entrained in a fluid flow and inferring the fluid velocity. A volume dedicated to the delineation of sources of error (11) examines in great detail the factors which should be considered in designing an experiment.

The approach taken here was to compare an LDA measurement of the mean velocity and turbulent intensity with a corresponding hot wire measurement at the same position and operating condition. The agreement of mean velocity was within $\pm$ 2.5% and the agreement of turbulent intensity was within $\pm$ 8%, i.e.

$$\langle U \rangle = \bar{U}(1 \pm 0.025) \text{ and}$$

$$\frac{s}{\langle U \rangle} = \frac{\sqrt{\overline{u^2}}}{\bar{U}} (1 \pm 0.08) .$$

4) The sample means and sample variances from the velocity histograms were determined by a "best fit" between a normal probability density function overlaid on the velocity histogram on a computer graphics terminal. With the freedom to vary the mean, μ, and variance, σ^2, of the normal density function as well as the upper and lower velocity limits outside of which the histogram data was discarded, the means μ and $\langle U \rangle$ and variances σ^2 and s^2 could be rapidly brought to convergence. Whether one has included bad data (noise) or excluded good data (valid Doppler signals) by this procedure is a matter of conjecture at this time and is a subject for future study. For example, the data might be subjected to a χ^2 "goodness of fit" criteria.

The values of turbulent intensity evaluated here are considered to be within $\pm$ 10% of their true value.

5) From both a consideration of the accuracy of the aperture micrometer drive and the motion of the combustion rig as the temperature and pressure of the rig approach their equilibrium values, errors in the spatial location of the measurement volume within the annulus are estimated to be within 10% of the aperture diameter imaged on the annulus height, i.e.

$r = r \pm 10\%$ (aperture diameter x collecting lens magnification)

$r(\text{mm}) = r(\text{mm}) \pm 0.10$ (0.275 mm x 10)

$r(\text{mm}) = r(\text{mm}) \pm 0.275$ mm

APPENDIX B

GRAPHICS-TERMINAL ANALYSIS

The values of the mean and variance of an LDA velocity histogram from a counter-processor with limited noise rejection capability in the presence of stray background radiation are not well-defined. Attempting to extract the mean and variance with some degree of confidence led to the following technique.

The output data from the counter-processor is tabulated by a laboratory digital computer in the form $n(U)/N$ vs. U,

where: U = particle velocity

$n(U)$ = number of particles with velocity U in bandwidth ΔU

$N = \Sigma\, n(U)$

$\frac{n(U)}{N}$ is hypothesized to be equivalent to the probability that the velocity $\hat{U}$ lies between U and $U + \Delta U$, i.e.

$$\frac{n(U)}{N} = P(U \leq \hat{U} \leq U + \Delta U)$$

From statistical theory

$$P(x \leq X \leq x + dx) = dF(x) = f(x)dx$$

and

$$\int dF(x) = F(x) = \int f(x)dx$$

with the following properties

$$\int_{-\infty}^{\infty} f(x)dx = 1, \quad \int_{a}^{b} f(x)dx = F(b) - F(a) = P(a \leq x \leq b)$$

where: $F(x)$ = cumulative distribution function

$f(x)$ = probability density function

Assuming that the turbulent flow through the combustor is a stationary, random process and that the individual measurements are normally distributed with mean μ and variance σ^2 (after the elimination of spurious data due to noise), a fit of the data to the standard normal probability density function should yield an estimate of μ and σ^2. In practice however, particularly in the presence of a high noise level, a subjective determination of which data constitutes noise and which is the desired data is required.

The standard normal probability density function

$$f(x) = \frac{e^{-x^2/2}}{\sqrt{2\pi}}$$

is transformed by a change of variable to

$$f(z) = \frac{e^{-z^2/2}}{\sqrt{2\pi}}$$

where: $z = \frac{U-\mu}{\sigma}$ and $dz = \frac{dU}{\sigma}$

so that

$$\int_{-\infty}^{\infty} f(z)dz = \int_{-\infty}^{\infty} \frac{e^{-(U-\mu)^2/2\sigma^2}}{\sigma\sqrt{2\pi}} dU = 1$$

or

$$f(z)\ \Delta z = \frac{e^{-(U-\mu)^2/2\sigma^2}}{\sigma\sqrt{2\pi}} \Delta U = P(U \leq \hat{U} \leq U + \Delta U)$$

$$= \frac{n(U)}{N}$$

The function

$$\frac{e^{-(U-\mu)^2/2\sigma^2}}{\sigma\sqrt{2\pi}} \quad \text{vs. } U$$

is overlaid on the data plotted as

$$\frac{1}{\Delta U} \quad \frac{n(U)}{N} \text{ vs. } U$$

on a computer graphics terminal. Values of μ and σ are varied to fit the data in the region of the estimated mean velocity. Data lying outside the interval $\mu + 3\sigma$ are discarded and a comparison is made between the "best fit" values of μ and σ^2 and the calculated values of sample mean $\langle U \rangle$ and sample variance s^2 from the remaining data.

where:

$$\langle U \rangle = \frac{\Sigma\, n(U)\; U}{N}$$

and

$$s^2 = \frac{\Sigma\, n(U)\; [U - \langle U \rangle]^2}{N-1}$$

With the additional freedom to vary the upper and lower velocity limits of truncation, the values of μ and $\langle U \rangle$ and σ and s may be rapidly brought to convergence.

The values of mean velocity and turbulent intensity (σ/μ or $s/\langle U \rangle$) presented here were determined in this manner. For example, see the following sketch for the Flight Idle-Burning, $r = 7.10$ mm data of Table 3.

Flight Idle-Burning, r = 7.10 mm

μ = 79.0 m/s, σ = 5.50 m/s

σ/μ = 6.96%

U_{upper} = 94.0 m/s, U_{lower} = 64.0 m/s

<U> = 79.0 m/s, s = 5.61 m/s

$s/_{<U>}$ = 7.10%

N = 820

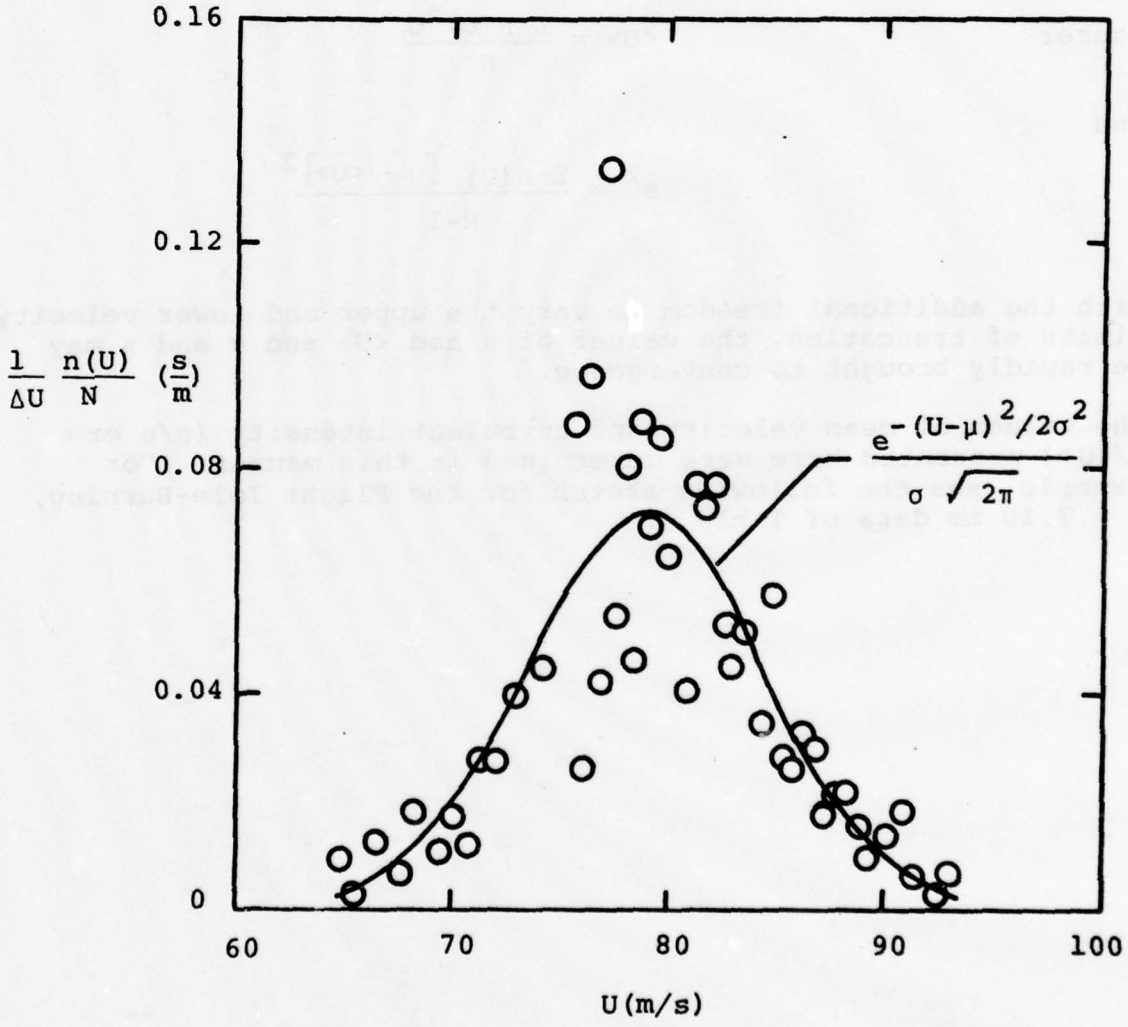

APPENDIX C

TANGENTIAL VELOCITY MEASUREMENT TECHNIQUE

The LDA indicates the velocity component in the plane of the two intersecting beams which establish the measurement volume and effectively set up a fringe system normal to this plane. The relation of the measured parameters to the orientation of the beams is shown below with the following nomenclature.

U_i	= instantaneous axial velocity
$U_i = \bar{U} + u$	= axial mean velocity + axial fluctuating velocity
V_i	= instantaneous tangential velocity
$V_i = \bar{V} + v$	= tangential mean velocity + tangential fluctuating velocity
$\overline{u^2}$, $\overline{v^2}$, $\overline{uv}$	= time averaged products of the fluctuating velocities
U_{m_j}	= measured particle velocity with fringe orientation j
$\langle U_{m_j} \rangle$	= ensemble averaged particle velocity, the sample mean of a velocity histogram with fringe orientation j
s_j^2	= variance of a velocity histogram with fringe orientation j

Case 1.

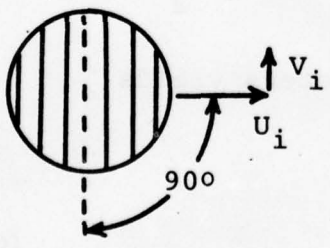

$$U_{m_1} = U_i$$

$$\langle U_{m_1} \rangle = \bar{U}$$

$$s_1^2 = \overline{u^2}$$

Case 2.

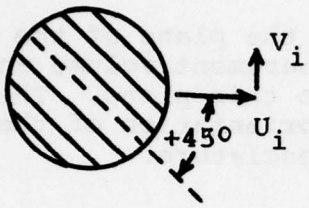

$$U_{m_2} = \frac{1}{\sqrt{2}} (U_i + V_i)$$

$$\langle U_{m_2} \rangle = \frac{1}{\sqrt{2}} (\bar{U} + \bar{V})$$

$$s_2^2 = \frac{\overline{u^2} + 2\overline{uv} + \overline{v^2}}{2}$$

Case 3.

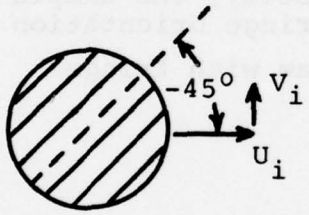

$$U_{m_3} = \frac{1}{\sqrt{2}} (U_i - V_i)$$

$$\langle U_{m_3} \rangle = \frac{1}{\sqrt{2}} (\bar{U} - \bar{V})$$

$$s_3^2 = \frac{\overline{u^2} - 2\overline{uv} + \overline{v^2}}{2}$$

Rearranging the preceding measured parameters yields

$$\bar{U} = \langle U_{m_1} \rangle = \frac{\langle U_{m_2} \rangle + \langle U_{m_3} \rangle}{\sqrt{2}} \qquad (C.1)$$

$$\overline{v} = \frac{\langle U_{m_2} \rangle - \langle U_{m_3} \rangle}{\sqrt{2}} \tag{C.2}$$

$$\overline{u^2} = s_1^2 \tag{C.3}$$

$$\overline{uv} = \frac{s_2^2 - s_3^2}{2} \tag{C.4}$$

$$\overline{v^2} = s_2^2 + s_3^2 - s_1^2 \tag{C.5}$$

$$\alpha = \tan^{-1} (\overline{V}/\overline{U}) \tag{C.6}$$

APPENDIX D

SYMBOLS

A	Annulus cross-sectional area
$\dot{m}$	Mass flow rate
P_T	Inlet total pressure
P_s	Annulus static pressure
Δp	Total pressure drop across the combustor
Q	Volumetric flow rate
r	Radial location in the annulus, r = 0 corresponds to the centerbody surface
R	Gas constant
s^2	Sample variance of a velocity histogram
T	Temperature
U_i	Instantaneous velocity in the axial direction
$\overline{U}$	Time-averaged axial velocity
$<U>$	Sample mean velocity of a histogram
ΔU	Velocity bandwidth dependent on the counter-processor resolution
u	Fluctuating velocity in the axial direction
$\overline{V}$	Time averaged tangential velocity
$w_{\dot{m}}, w_T, w_{P_T}, w_{\Delta p}, w_Q$	Uncertainties in the measured parameters; $\dot{m}$, T, P_T, Δp, and the calculated Q
$s/_{<U>}, \sqrt{\overline{u^2}}/\overline{U}, \sigma/_{\mu}$	Turbulent intensity, all assumed equivalent
α	Swirl angle
μ, σ^2	Assumed mean and variance in a normal probability density function to "best fit" a velocity histogram
ρ	Density

REFERENCES

1. van der Hegge Zijnen, B. G., "Heat Transfer From Horizontal Cylinders to Turbulent Air Flow", Applied Scientific Research, Vol. 7, pp. 205-223, 1958.

2. Turner, A. B., "Local Heat Transfer Measurements on a Gas Turbine Blade", Journal of Mechanical Engineering Science, Vol. 13, pp. 1-12, 1971.

3. Simonich, J. C. and Bradshaw, P., "Effect of Free-Stream Turbulence on Heat Transfer Through a Turbulent Boundary Layer", Journal of Heat Transfer, Vol. 100, No. 4, pp. 671-677, 1978.

4. Schaefer, H. J., Koch, B. and Pfeifer, H. J., "Application of LDV Techniques to High Speed Combustion Flows", International Congress on Instrumentation in Aerospace Simulation Facilities, Shrivenham, England, Sept. 1977.

5. Eckert, E.R.G., Goldstein, R. J. and Sparrow, E. M., "Heat Transfer Problems in Advanced Gas Turbines for Naval Applications", Annual Progress Report on Navy Contract N00014-76-C-0246, University of Minnesota, Aug. 1977.

6. Driscoll, J. F. and Pelaccio, D. G., "Laser Velocimetry Measurements in a Gas Turbine Research Combustor", Proceedings of the Third International Workshop on Laser Velocimetry, Purdue University, July 1978, pp. 158-165.

7. Edelman, R. B. and Harsha, P. T., "Current Status of Laminar and Turbulent Gas Dynamics in Combustors", Combustion Institute, Spring Meeting, Cleveland, Ohio, March 1977.

8. Durst, F., Melling, A. and Whitelaw, J. H., Principles and Practice of Laser-Doppler Anemometry, Academic Press, N.Y. N.Y., 1976.

9. Smith, K. O. and Gouldin, F. C., "Experimental Investigation of Flow Turbulence Effects on Premixed Methane-Air Flames", AIAA Aerospace Sciences Meeting, Los Angeles, CA, Jan. 1977.

10. Kline, S. J. and McClintock, F. A., "Describing Uncertainties in Single-Sample Experiments", Mechanical Engineering, Vol. 75, pp. 3-8, 1953.

11. Buchave, P., et.al., Editors, The Accuracy of Flow Measurements by Laser Doppler Methods, Proceedings of the LDA-Symposium, Copenhagen, 1975.

Table 1. Combustor Operating Conditions

	Burner Inlet Temperature (K)	Burner Inlet Pressure (kPa)	Air Flow (kg/s)	Burner Outlet Temperature (K)
Flight Idle	425	314	0.77	877
30% Power	472	434	1.03	1000
90% Power	562	689	1.50	1292
Take Off	572	724	1.52	1342

Table 2. Laser Anemometer Velocity Data

	Radial Location (mm)	Mean Velocity (m/s)	Turbulent Intensity (percent)
Flight Idle, Isothermal	2.02	39.5	-
	4.56	40.1	6.73
	7.10	39.5	6.71
	9.64	39.2	6.63
	12.18	39.6	6.57
30% Power, Isothermal	4.56	40.5	-
	7.10	42.3	8.27
	9.64	41.5	8.43
	12.18	41.8	8.13
90% Power, Isothermal	7.10	48.3	8.74
	8.37	47.6	9.24
	9.64	46.4	9.70
	12.18	45.3	9.05
Take Off, Isothermal	5.83	46.6	8.80
	7.10	46.5	9.46
	9.64	46.6	10.09
	12.18	44.1	10.43
Flight Idle, Burning	4.56	80.0	6.88
	7.10	79.0	6.96
	9.64	79.5	6.29
	12.18	78.0	6.41
30% Power, Burning	7.10	85.0	9.18
	9.64	86.0	7.09
	12.18	81.0	7.41
90% Power, Burning	7.10	102.0	9.80
	9.64	101.0	9.70
	12.18	102.0	9.31
Take Off, Burning	7.10	104.0	-

Table 3. Typical Histogram Data
(Flight Idle-Burning, r = 7.10 mm)

n(U)	U(m/s)	n(U)	U(m/s)	n(U)	U(m/s)	n(U)	U(m/s)
1	104.32	14	80.84	2	62.26	2	46.51
1	103.62	18	80.42	5	61.76	1	45.15
1	102.93	22	80.00	7	61.27	1	44.88
1	99.61	29	79.59	4	60.79	2	44.62
2	98.97	23	79.18	1	60.31	1	44.37
1	98.34	29	78.78	3	59.84	2	44.11
1	97.11	15	78.38	3	59.38	1	43.86
2	96.50	26	77.98	9	58.93	1	43.62
5	94.15	17	77.59	2	58.48	2	43.13
2	93.58	42	77.20	3	58.05	1	42.89
3	93.01	13	76.82	3	57.61	1	42.65
1	92.46	30	76.44	2	57.19	1	41.96
2	91.90	8	76.06	2	56.76	1	41.73
3	91.36	40	75.69	6	56.35	2	41.51
8	90.82	33	74.95	4	55.94	2	41.28
6	90.29	26	74.23	1	55.54	2	41.06
5	89.77	23	73.52	4	55.14	2	40.00
4	89.25	22	72.83	2	54.75	1	39.79
7	88.74	15	72.15	3	54.37	1	38.22
9	88.23	15	71.48	3	53.99	2	37.84
9	87.73	6	70.83	4	53.61	1	37.48
7	87.23	9	70.18	2	53.24	2	37.12
12	86.74	5	69.55	1	52.52	1	36.76
13	86.26	7	68.93	1	52.16	2	36.42
10	85.78	9	68.32	2	51.81	2	36.07
11	85.30	3	67.72	1	51.47	4	35.74
22	84.84	4	67.13	1	51.13	2	34.77
13	84.37	6	66.55	3	50.46	1	34.46
16	83.91	3	65.98	1	50.13	1	33.86
19	83.46	1	65.42	1	49.81	1	31.90
16	83.01	4	64.87	1	49.49	1	30.63
19	82.57	5	64.33	1	48.55	1	29.69
28	82.13	5	63.80	1	48.25	1	15.08
26	81.69	5	63.28	2	47.65		
27	81.26	7	62.76	3	47.36	995 = N	

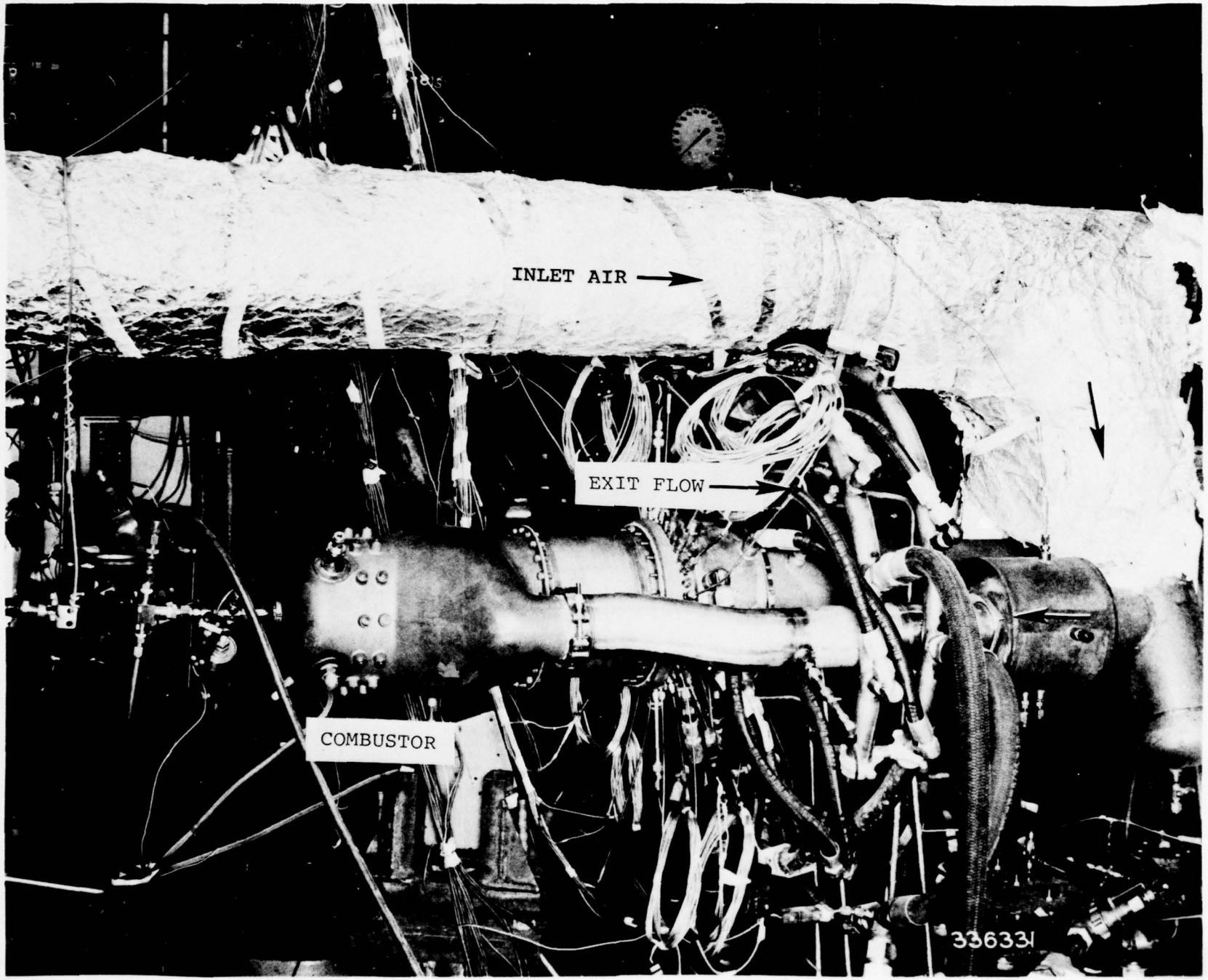

FIGURE 1. T63 COMBUSTION RIG

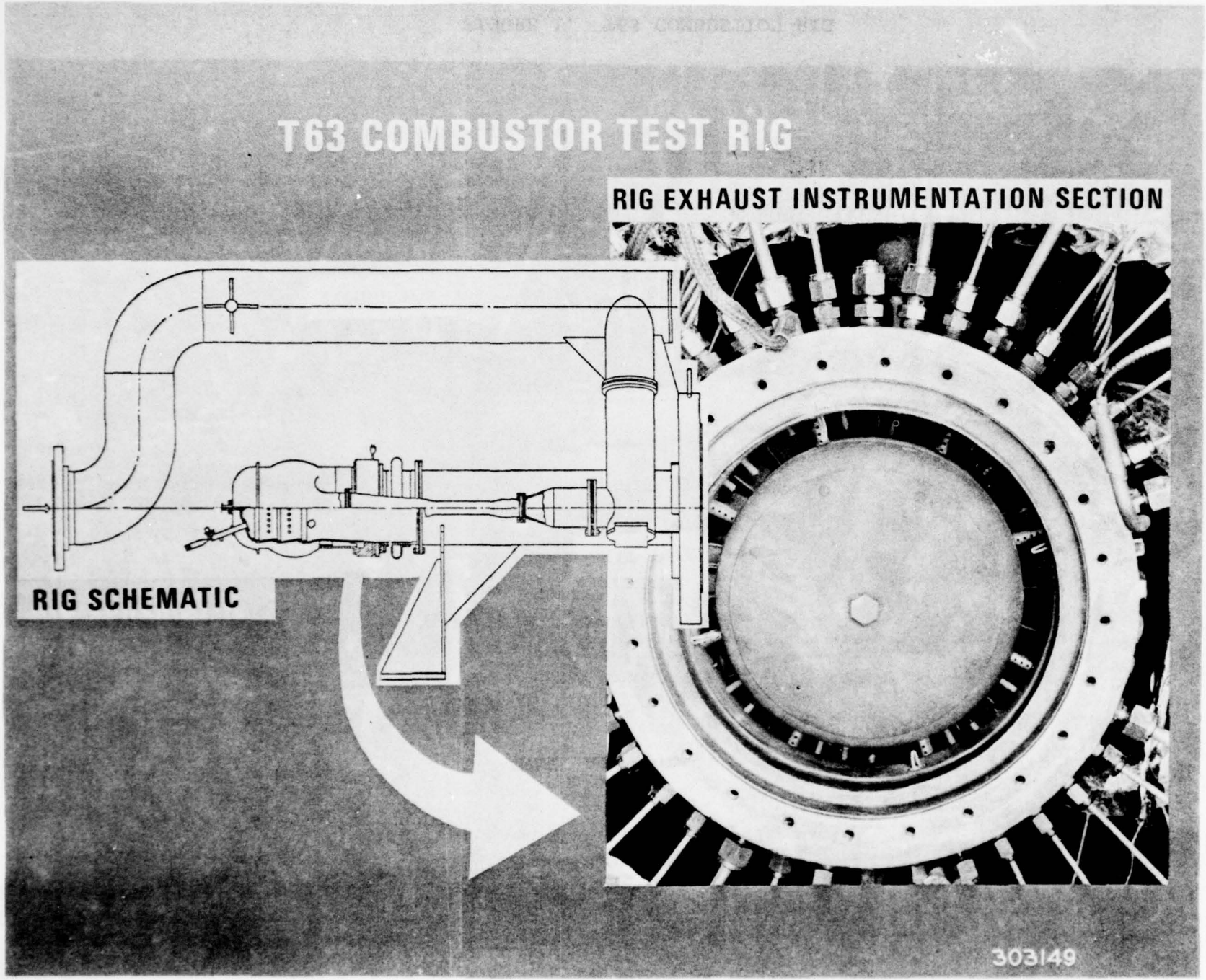

FIGURE 2. INSTRUMENTATION SPOOLPIECE

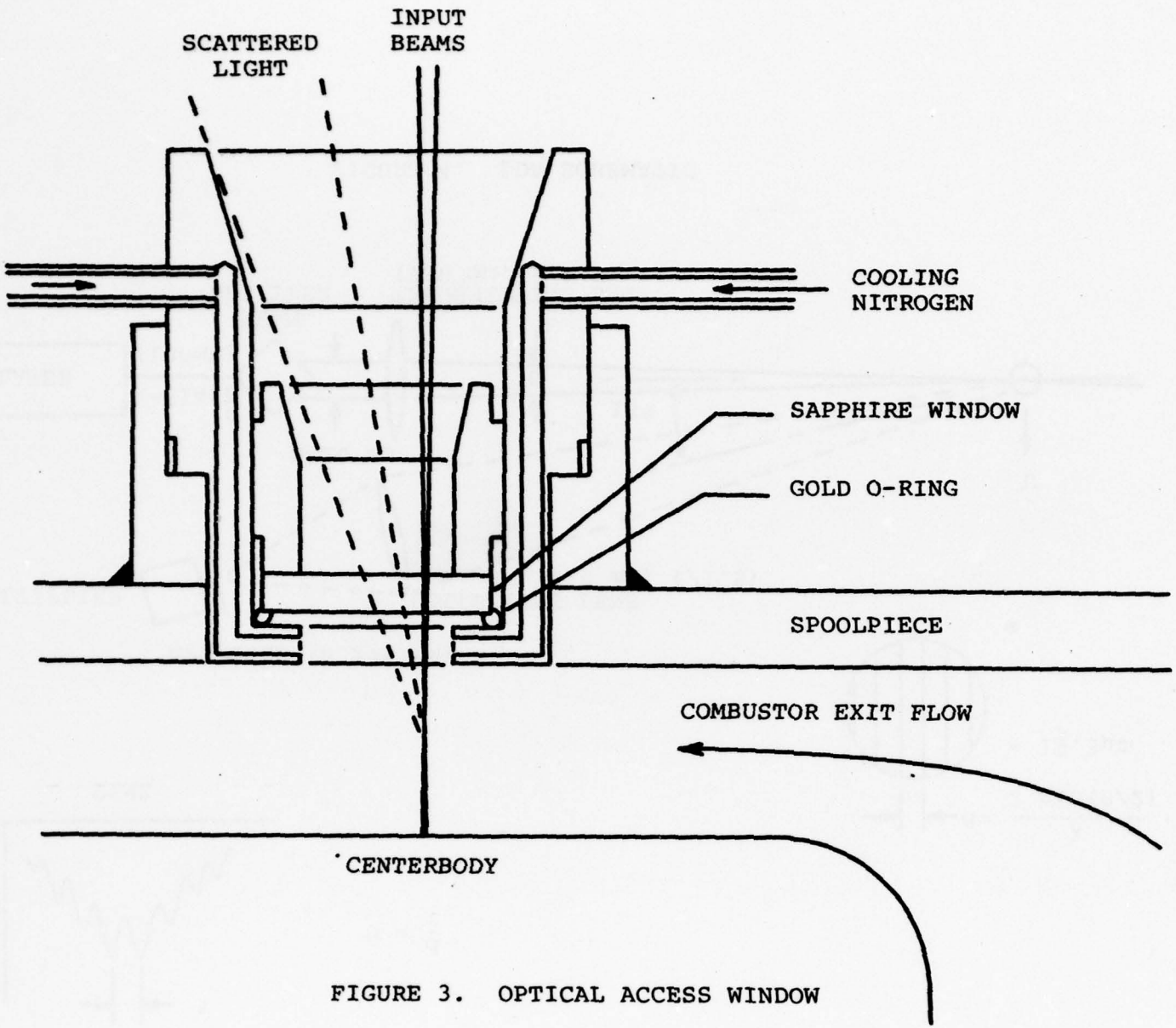

FIGURE 3. OPTICAL ACCESS WINDOW

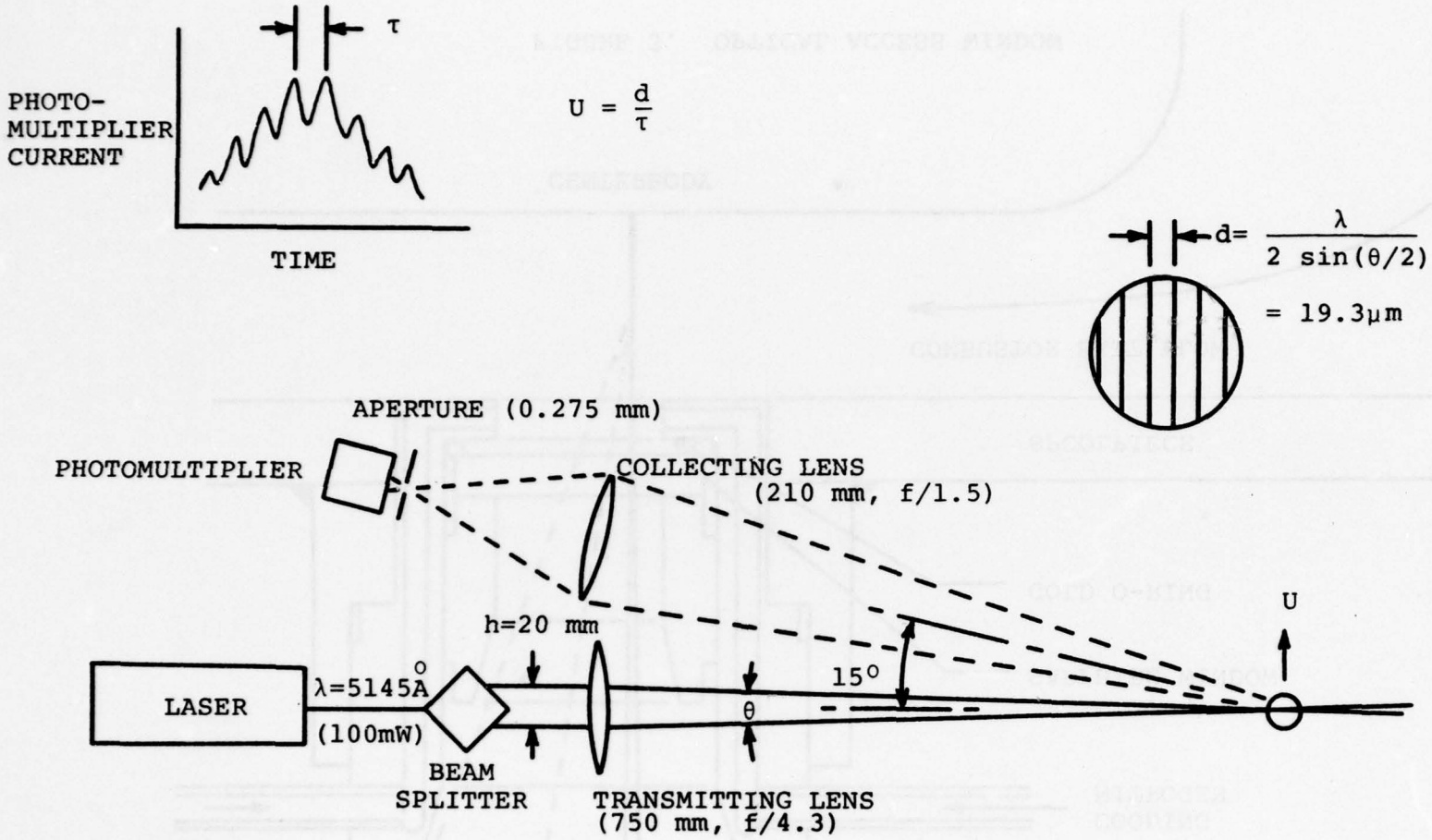

FIGURE 4. LDA SCHEMATIC

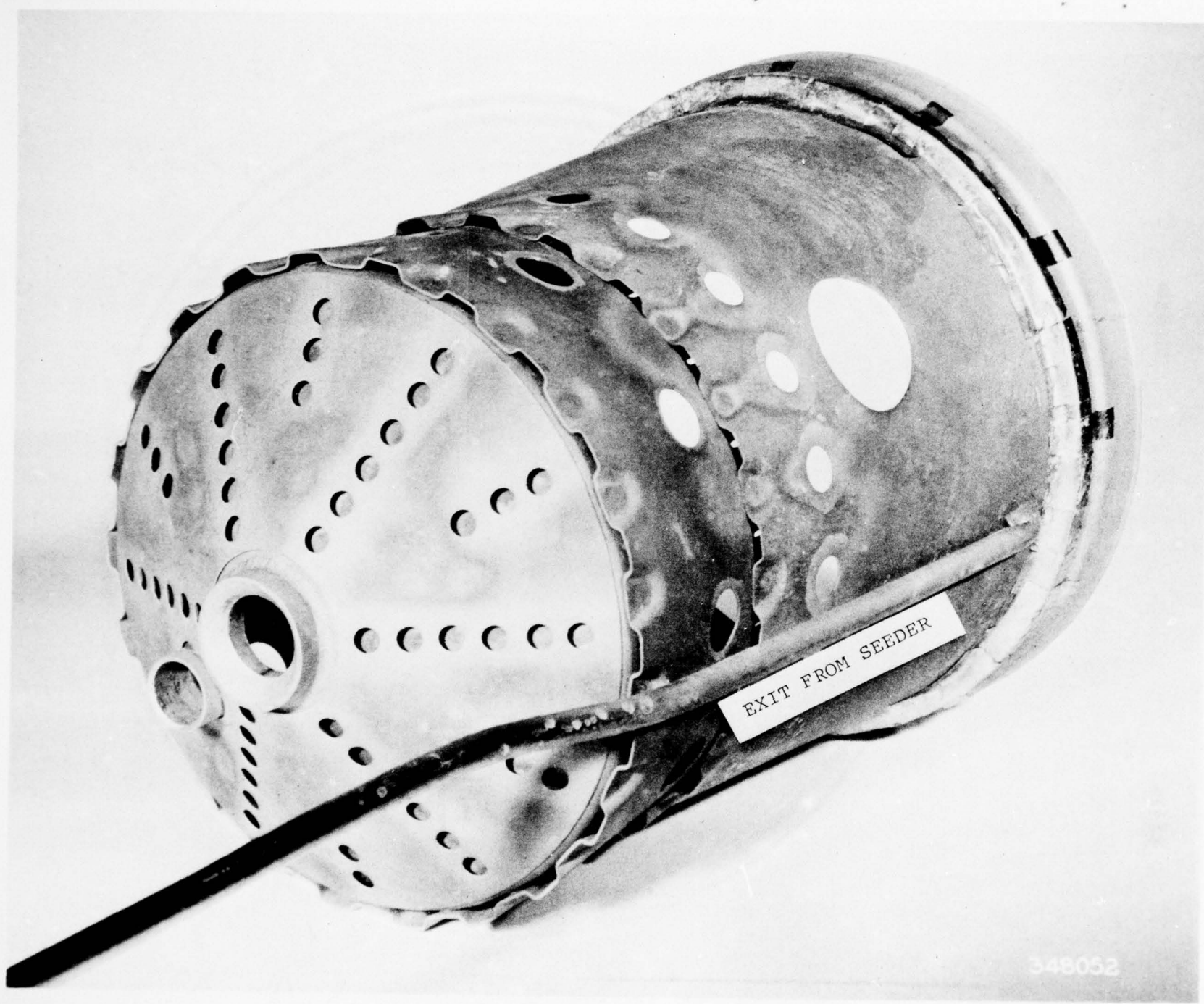

FIGURE 5. T63-C20 COMBUSTOR LINER

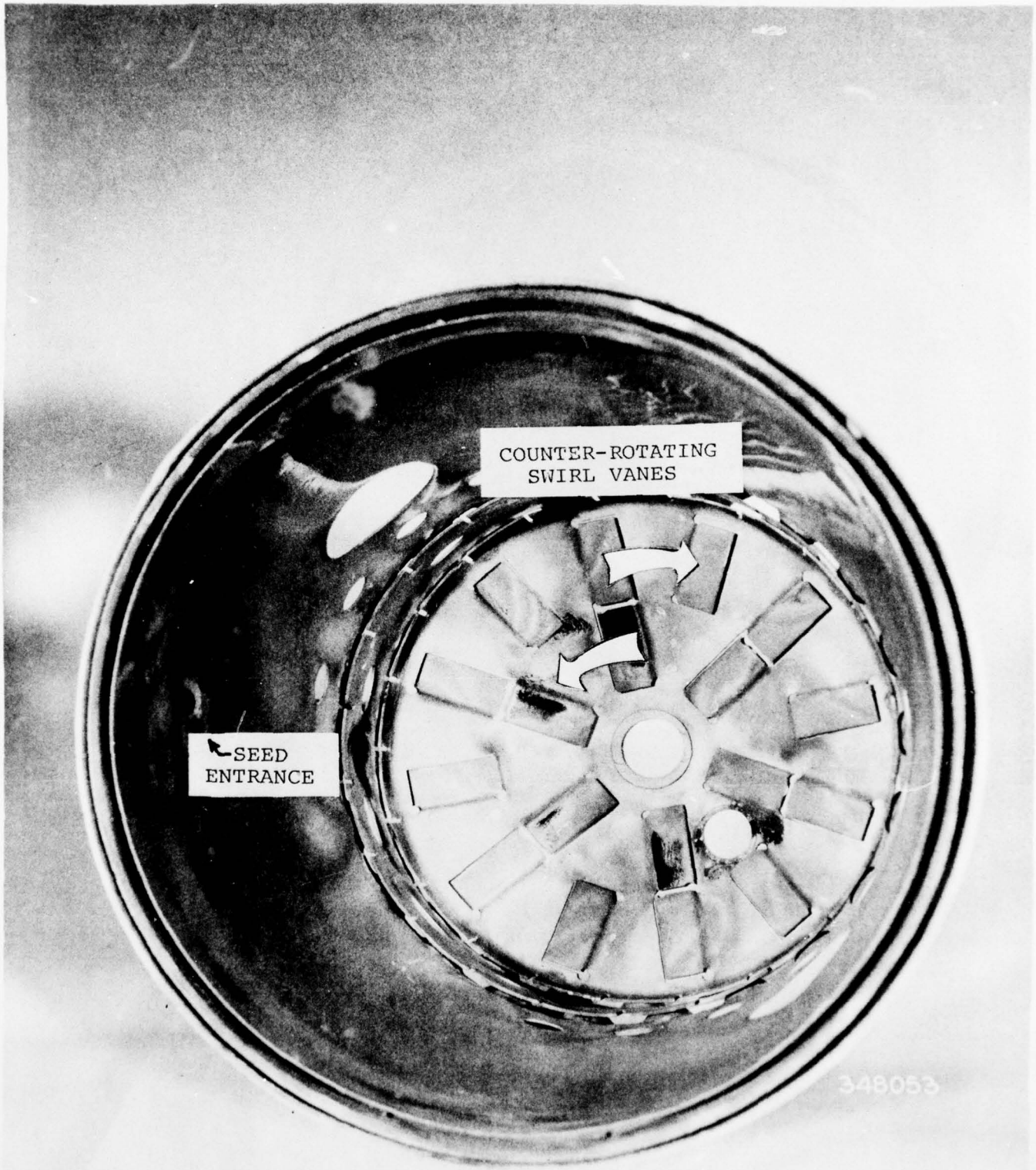

FIGURE 6. T63-C20 COMBUSTOR LINER

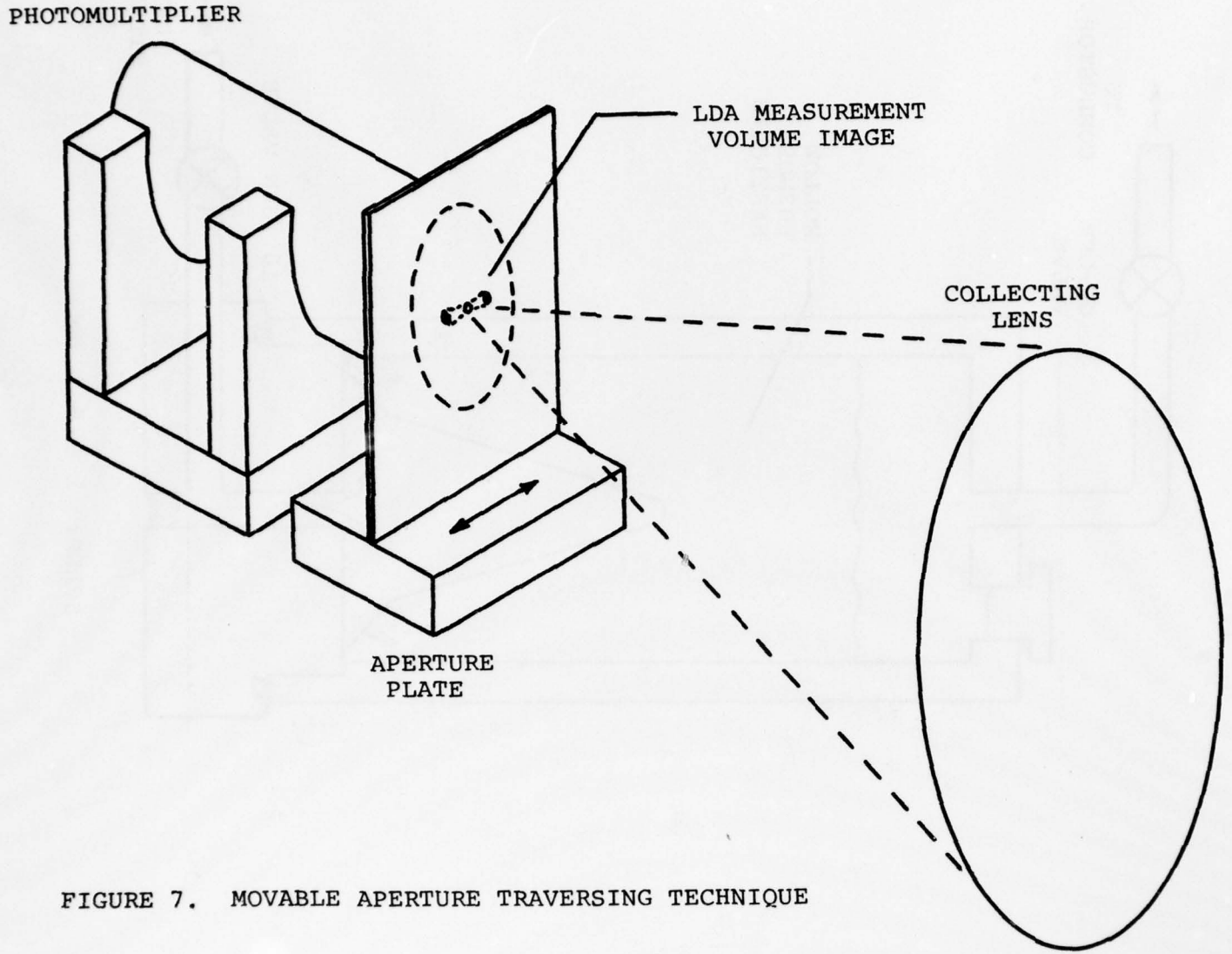

FIGURE 7. MOVABLE APERTURE TRAVERSING TECHNIQUE

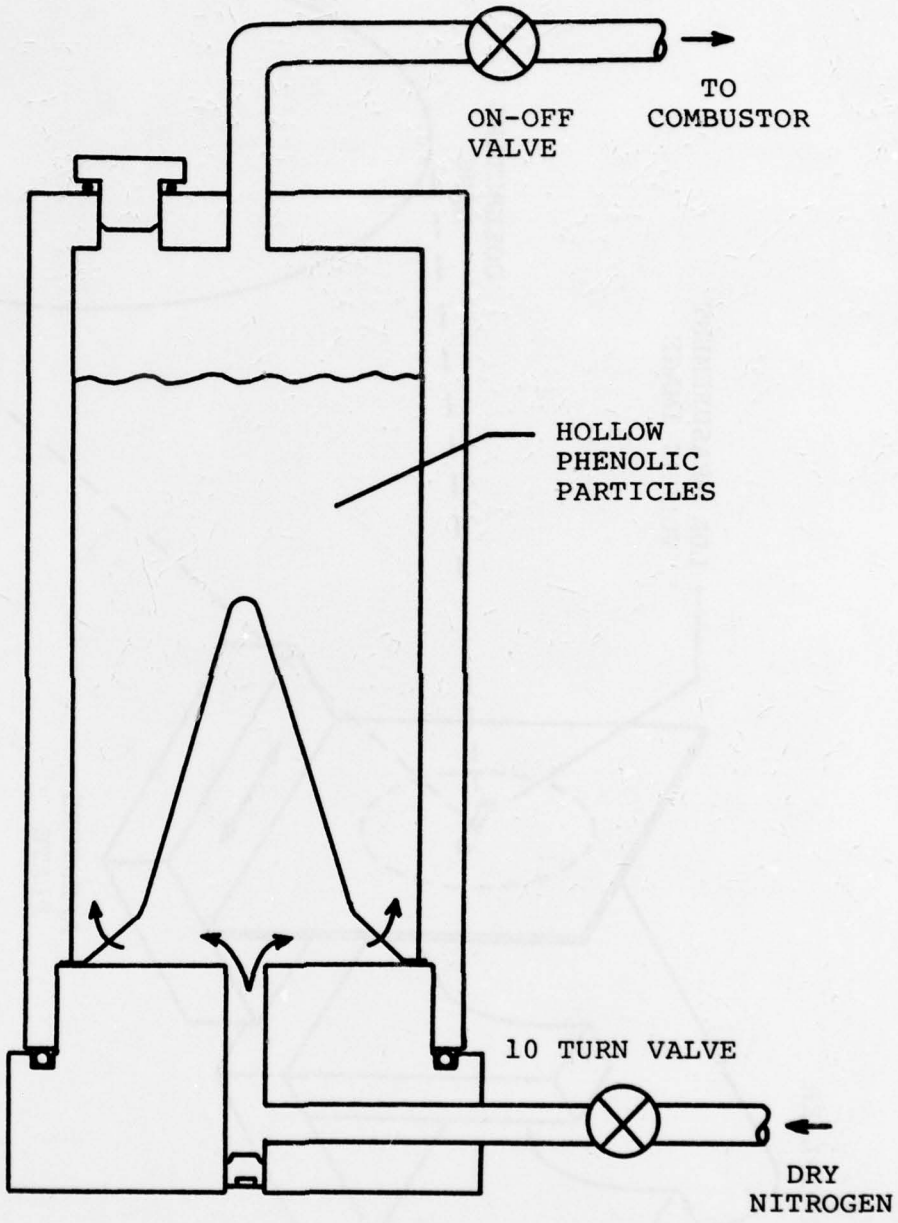

SCALE: 1 cm = 2 cm

FIGURE 8. SEEDER

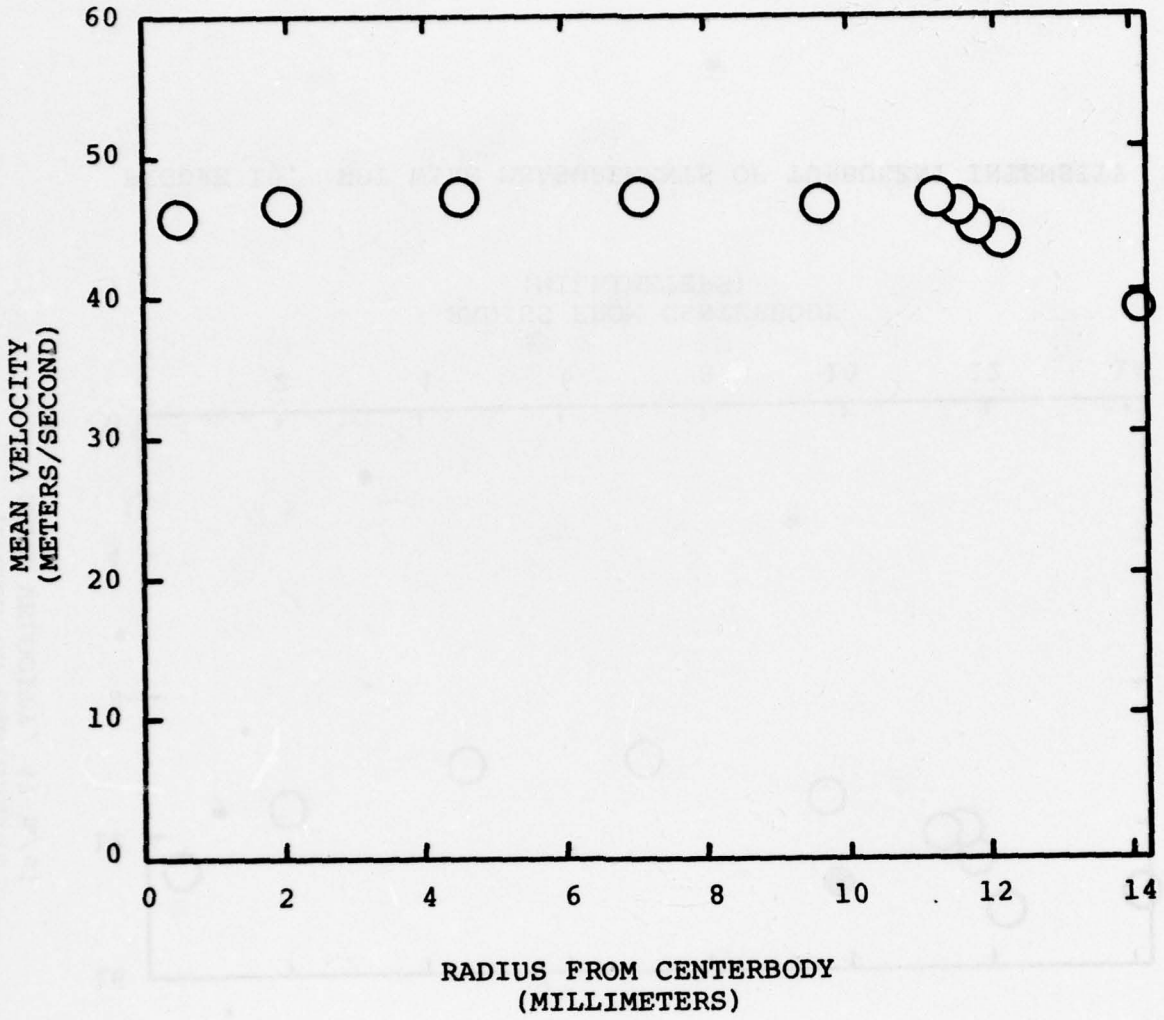

FIGURE 9. HOT WIRE MEASUREMENTS OF MEAN VELOCITY

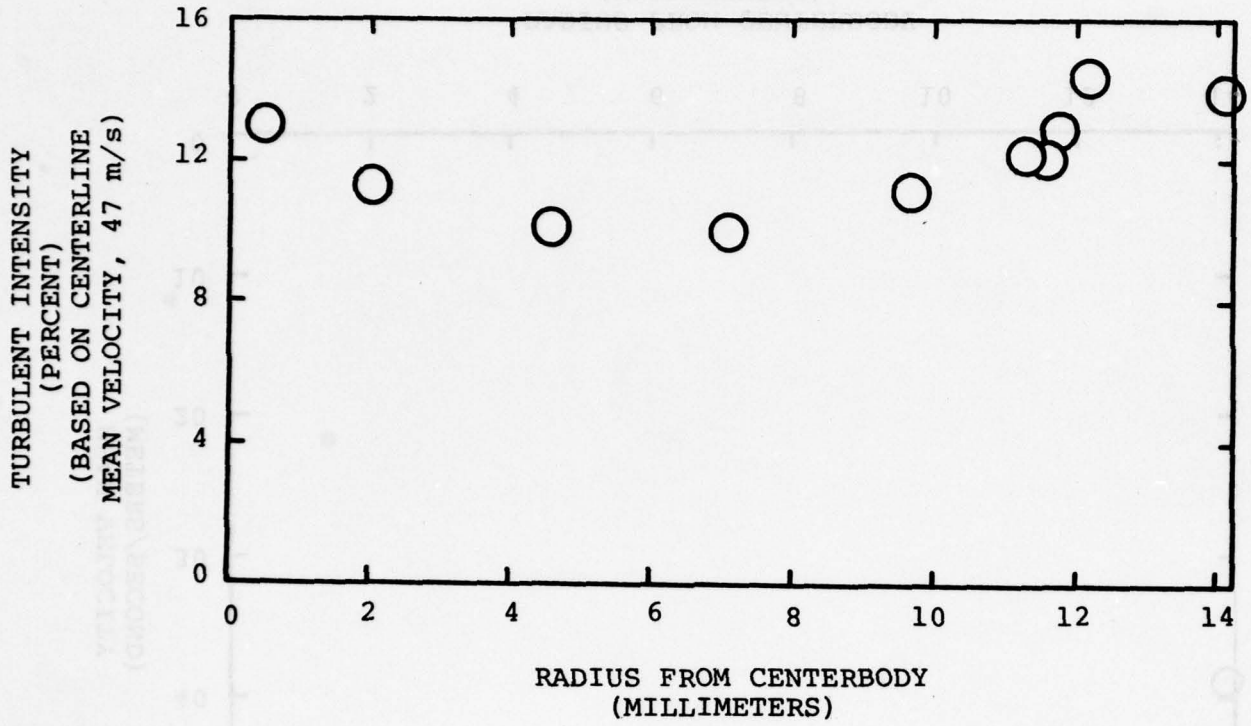

FIGURE 10. HOT WIRE MEASUREMENTS OF TURBULENT INTENSITY

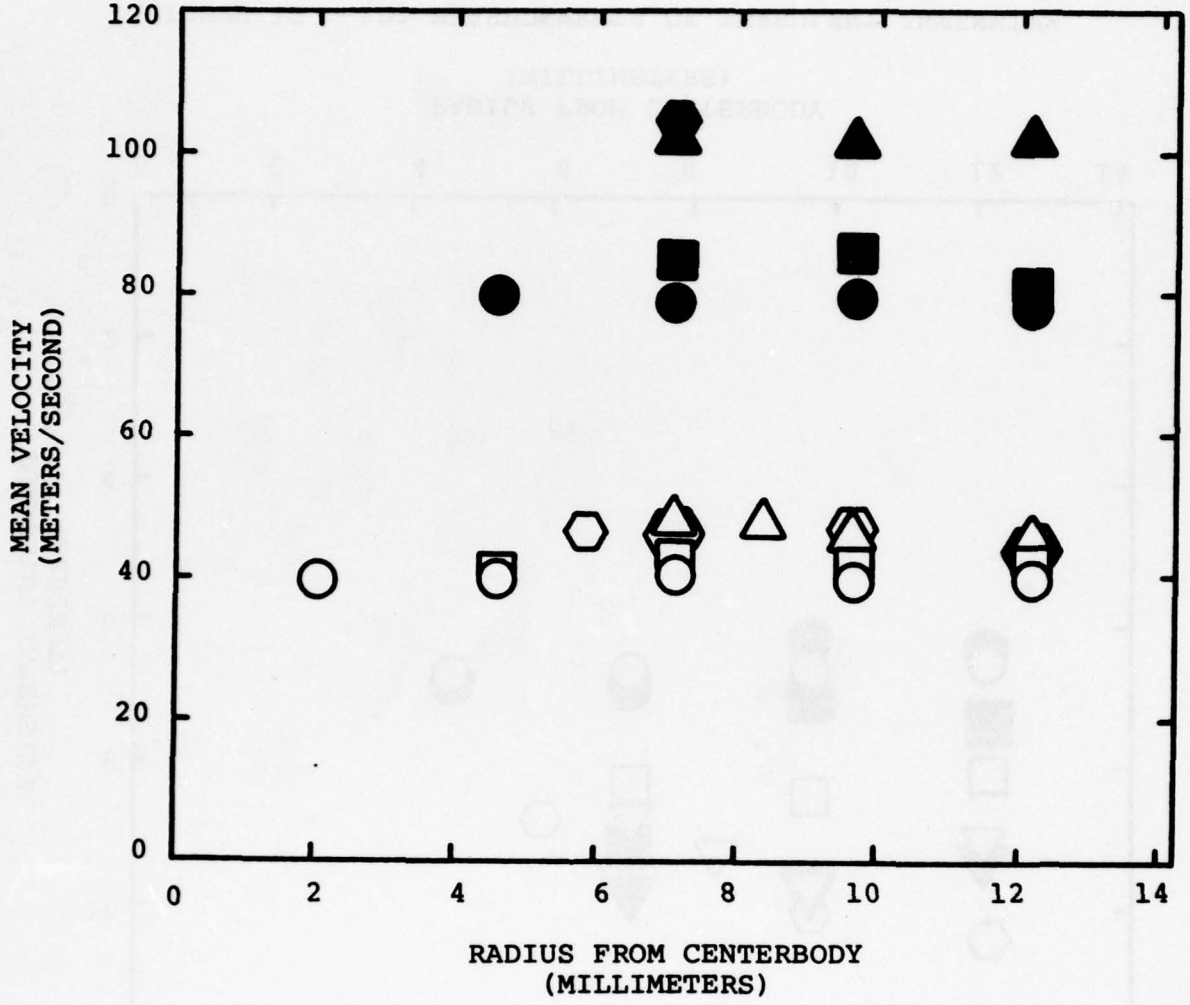

FIGURE 11. LDA MEASUREMENTS OF MEAN VELOCITY
(○ -IDLE, □ -30% POWER, △ -90% POWER, ⬡ -TAKEOFF,
OPEN SYMBOLS - ISOTHERMAL, CLOSED SYMBOLS - WITH COMBUSTION)

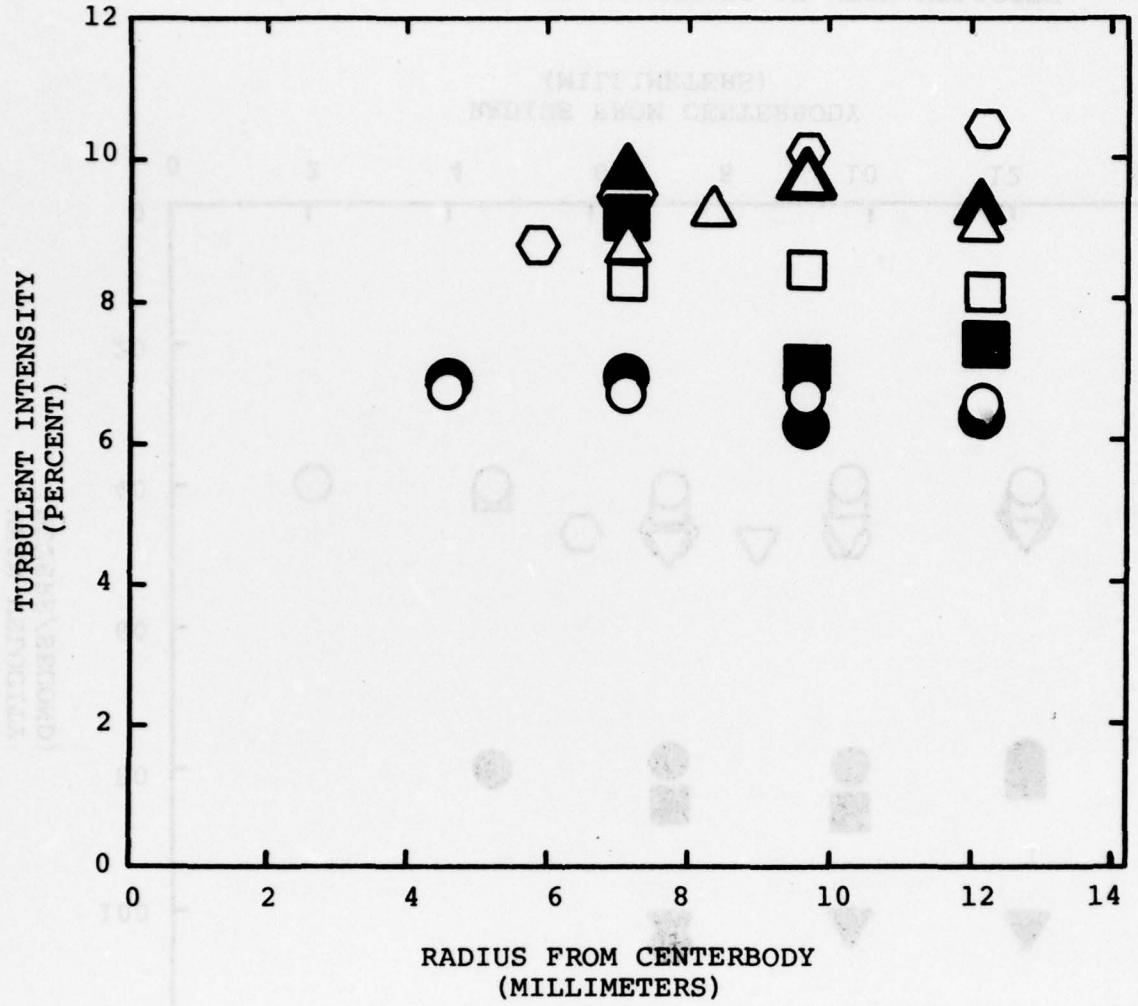

FIGURE 12. LDA MEASUREMENTS OF TURBULENT INTENSITY
(○-IDLE, □-30% POWER, △-90% POWER, ⬡-TAKE OFF,
OPEN SYMBOLS - ISOTHERMAL, CLOSED SYMBOLS - WITH COMBUSTION)

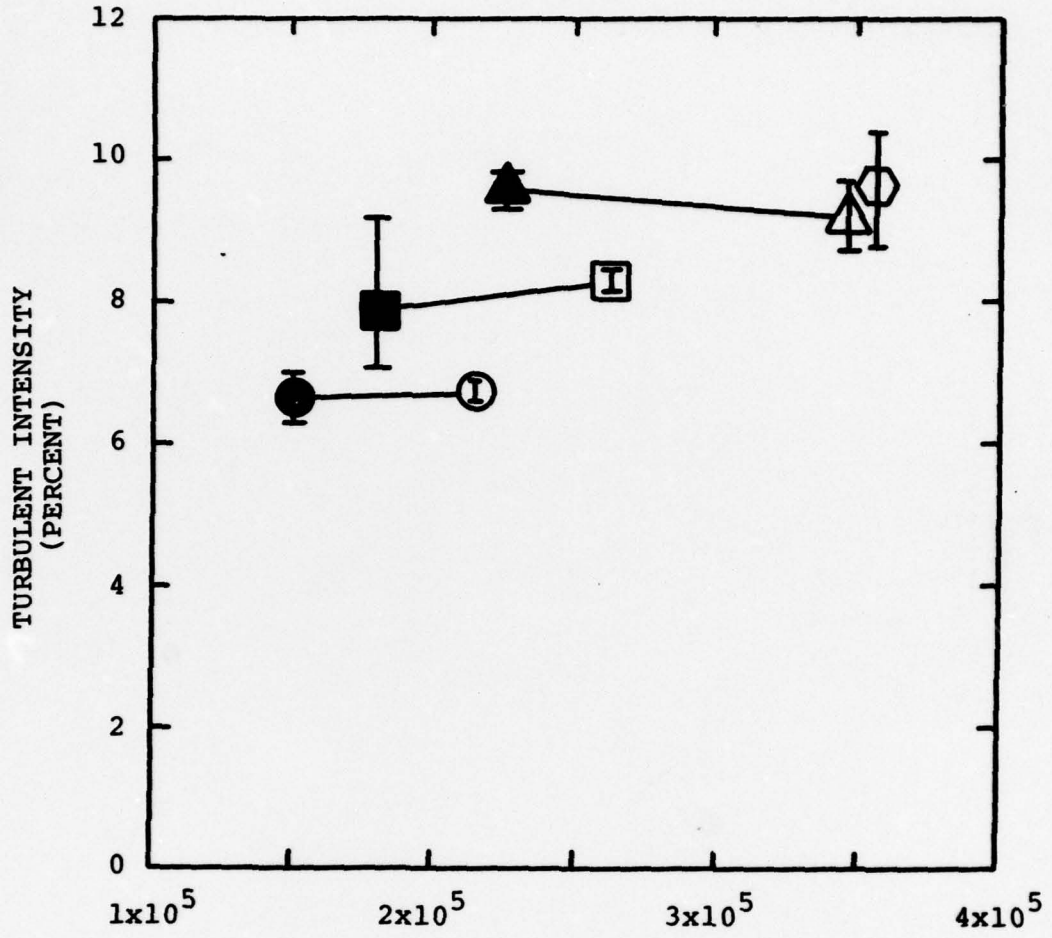

FIGURE 13. EFFECT OF INLET REYNOLDS NUMBER AND COMBUSTION ON TURBULENT INTENSITY
(○ -IDLE, □ -30% POWER, △ -90% POWER, ⬡ -TAKE OFF,
OPEN SYMBOLS - ISOTHERMAL, CLOSED SYMBOLS - WITH COMBUSTION)